HHS Public Access

Author manuscript

Brain Behav Immun. Author manuscript; available in PMC 2019 October 23.

Published in final edited form as:

Brain Behav Immun. 2011 March ; 25(3): 483–493. doi:10.1016/j.bbi.2010.11.011.

Constitutive and LPS-regulated expression of interleukin-18 receptor beta variants in the mouse brain

Silvia Alboni[1], **Claudia Montanari**[1], **Cristina Benatti**[1], **Johanna M.C. Blom**[2], **Maria Luisa Simone**[1], **Nicoletta Brunello**[1], **Federica Caggia**[1], **Gianluigi Guidotti**[1], **Maria Cecilia Garibaldi Marcondes**[3], **Manuel Sanchez-Alavez**[3], **Bruno Conti**[3], **Fabio Tascedda**[1]

[1]Department of Biomedical Sciences University of Modena and Reggio Emilia, Italy

[2]Department of Paediatrics University of Modena and Reggio Emilia, Italy

[3]Molecular and Integrative Neurosciences Department The Scripps Research Institute, La Jolla, CA, 92037

Abstract

Interleukin (IL)-18 is a pro-inflammatory cytokine that is proposed to be involved in physiological as well as pathological conditions in the adult brain. IL-18 acts through a heterodimer receptor comprised of a subunit alpha (IL-18Rα) required for binding, and a subunit beta (IL-18Rβ) necessary for activation of signal transduction. We recently demonstrated that the canonical alpha binding chain, and its putative decoy isoform, are expressed in the mouse central nervous system (CNS) suggesting that IL-18 may act on the brain by directly binding its receptor.

Considering that the co-expression of the beta chain seems to be required to generate a functional receptor and, a short variant of this chain has been described in rat and human brain, in this study we have extended our investigation to IL-18Rβ in mouse.

Using a multi-methodological approach we found that: 1) a short splice variant of IL-18Rβ was expressed in the CNS even if at lower levels compared to the full-length IL-18Rβ variants 2) the canonical IL-18Rβ is expressed in the CNS particularly in areas and nuclei belonging to the limbic system as previously observed for IL-18Rα, finally 3) we have also demonstrated that both IL-18Rβ isoforms are up-regulated in different brain areas three hours after a single lipopolysaccharide (LPS) injection suggesting that IL-18Rβ in the CNS might be involved in mediating the endocrine and behavioral effects of LPS.

Our data highlight the considerable complexity of the IL-18 regulation activity in the mouse brain and further support an important central role for IL-18.

Address correspondence to: Fabio Tascedda or Silvia Alboni Department of Biomedical Sciences, University of Modena and Reggio Emilia, Via Campi 287 41125 Modena, Italy. Phone: +390592055162, Fax: +390592055625, fabio.tascedda@unimore.it, silvia.alboni@unimo.it.

All authors declare that there are no conflicts of interest

Keywords

interleukin-18; lipopolysaccharide; brain; mouse; IL-18Rβ; splice variant

1. INTRODUCTION

Interleukin (IL)-18 is a pro-inflammatory cytokine with a pivotal role in innate as well as adaptive immunity (Okamura et al., 1998; Takeda et al., 1998). Several studies found that IL-18 is also produced and is biologically active in the CNS where it is proposed to participate in local inflammatory reactions but also to modulate autonomic functions and the sickness behavior (recently reviewed in Alboni et al., 2010). Yet, its mode of central action remains to be elucidated. IL-18 acts on cells of the immune system through binding to its heterodimer receptor (IL-18R) belonging to the interleukin 1 receptor/Toll like receptor superfamily. IL-18R consists of one ligand binding chain (IL-18Rα, also known as IL-18RI, IL-1Rrp or IL-1R5) and an accessory protein (IL-18Rβ, also known as IL-18RII, IL-18RαcP or IL-1R7) (Hoshino et al., 1999; Torigoe et al., 1997) essential for signal transduction (Sergi and Penttila, 2004). We recently demonstrated that the canonical α chain of the IL-18R (that we arbitrarily named IL-18Rα type I) is widely expressed in neurons throughout the mouse CNS (Alboni et al., 2009). Moreover, we demonstrate the *in vivo* expression in the mouse brain of a short transcript for the α chain (arbitrarily named IL-18Rα type II) lacking the intracellular Toll/IL-1 receptor (TIR) domain is required for IL-18 signaling and is thus proposed to be a decoy receptor (Alboni et al., 2009). Together, these findings provided evidence for a possible direct action of IL-18 on neurons and suggest that its activity may be modulated by regulating the levels of the decoy isoform.

To further investigate this possibility and the biology of central IL-18 we extended our studies to determine the central distribution of the IL-18Rβ subunit that is necessary to activate IL-18 signaling (Born et al., 1998; Cheung et al., 2005). We also investigated in the mouse brain the existence of splice variants of IL-18Rβ similar to those described in rat and human, and proposed to be soluble negative regulator of IL-18 action (Andre et al., 2003; Fiszer et al., 2007). Finally, we also analyzed the effect of peripheral injection of bacterial endotoxin lipopolysaccharide (LPS) on the central expression of the IL-18 system components. LPS is a potent activator of pro-inflammatory cytokines and a peripheral model of sickness syndrome characterized by behavioral and physiological changes regulated centrally including fever, anorexia, lethargy, anxiety, depressed mood, cognitive impairment and reduced social interaction (Dantzer., 1998; 2008; Frenois et al., 2007; Gatti and Bartfai, 1993; Layé et al., 1994; Meyer et al., 1994; Quan et al., 1999).

2. METHODS

2.1 Animals and treatments

Two month old C57BL6/J male mice were used in this study. Animals were housed in polycarbonate cages (28 × 17 × 12 cm) with *ad libitum* access to food and water throughout the study, maintained under a 12:12 light-dark cycle in an ambient temperature of 21 ± 3 °C with relative humidity controlled. Animals were checked for signs of discomfort as indicated

by animal care and use guidelines (National Academy of Sciences. Guide for the care and use of laboratory animals, 1998, “Guidelines for the Care and Use of Mammals in Neuroscience and Behavioral Research” (National Research Council 2003)). All procedures were carried out in accordance with the EC guidelines (EEC Council Directive 86/609 1987), Italian legislation on animal experimentation (Decreto Legislativo 116/92) and The Scripps Research Institute Institutional Animal Care and Use Committee.

LPS (100 μg at 1 μg/μl strain 055:B5, Sigma Aldrich L2880) were injected intraperitoneally (i.p.) (n=3) and an equal volume of vehicle (saline) was used as a control (n= 3). Tissues were harvested 3 hrs after injection and stored at −80°C until RNA extraction.

2.3 *In situ* hybridization

Determination of IL-18Rβ mRNA in the CNS was performed by non-isotopic *in situ* hybridization (ISH) using a specific DIG-labeled anti-sense riboprobe common to both isoforms, and a sense probe as negative control. cDNA [nt 759–1137 (NCBI GenBank accession number: NM_010553)] for mouse IL-18Rβ was subcloned into pDrive Cloning Vector (Quiagen®, Hilden, Germany) in order to obtain a template for the *in vitro* transcription of cRNAs [antisense (using BamH I restriction site); sense (using Hind III restriction site)]. Probes (antisense –AS- and sense –S) for IL-18Rβ to be employed in *in situ* hybridization assay, were synthesized using the DIG-RNA labeling kit (La Roche Diagnostics, Mannheim, Germany) according to the manufacturer’s instructions [SP6 polymerase for IL-18Rβ AS probe – T7 polymerase for IL-18Rβ S probe].

For *in situ hybridization* mice were anaesthetized by isoflurane inhalation and perfused transcardially with heparinized (5.000 U.I./L) saline followed by perfusion with ice-cold 4% paraformaldehyde in PBS pH 7.4. After fixation, their brains were rapidly removed and post fixed in the same fixative solution for 4 hrs, and then cryoprotected in a 30% sucrose solution in phosphate buffer pH 7.4. *In situ* hybridization was carried out as previously described on 40-μm thick serial coronal sections (see Alboni et al., 2009 for further details).

The specificity of the hybridization signals in the brain regions were confirmed by comparing sections hybridized with the antisense probe to those hybridized with the sense probe. No hybridization signals were detectable in consecutive sections hybridized with the sense probe. The relative intensities of the IL-18Rβ mRNA in various brain regions were evaluated in hybridized coronal sections via transillumination microscopy by al least two independent investigators. Anatomical brain regions and nomenclature were those of the Franklin and Paxinos mouse brain atlas (Franklin and Paxinos, 1997). The staining intensities used in Table I were arbitrarily assigned to reflect the following: −, not detectable; +/−, very low signal; +, weak signal; +(++), a weak to moderate signal; ++, moderate signal; ++(+++) a moderate to strong signal; +++, strong signal. Figures were prepared using Adobe Photoshop 7.0.1 with minor adjustments to contrast and brightness.

2.4 Immunohistochemistry

Mice were sacrificed upon perfusion with 0.2% EDTA-containing PBS, under isoflorane. Brains were processed immediately after perfusion. Brains were removed and bisected in midsagittal plane, fixed in 10% formalin, embedded in paraffin, and cut into 5 μm sections.

Following a 40 min 95ºC steam bath in 10mM citrate buffer (pH6.38) for antigen retrieval, representative sections of brain (plus spleen controls) were immunohistochemically stained, using an anti IL-18Rβ antibody (BAF1520, R&D Systems, Minneapolis, MN) followed by biotinylated anti-goat IgG secondary antibody (Vector Labs, Burlingame, CA) and streptavidin HRP (Invitrogen, San Diego, CA), and was developed with NovaRed (Vector Labs). Sections were counterstained with Gill's hematoxylin (Invitrogen). Images from cells were visualized and acquired using a Zeiss (Oberkochen, Germany) Axiovert 200 inverted microscope at 20 and 32× magnification and captured by using the Zeiss Axiocam HRC associated with the Zeiss Axiovision 2.0.5 software package. Controls performed by omitting primary antibodies were negative.

2.5 RNA extraction and retro transcription

Total RNA extraction was performed using TRIzol® reagent (Sigma®, St. Louis, MO, USA) followed by a clean-up step on Qiagen RNeasy Spin Column and DNAse treatment to remove genomic contamination following the manufacturer's instructions (Qiagen®, Hilden, Germany). 1 μg of total RNA was reverse transcribed with High Capacity cDNA Reverse Transcription Kit (Life Technologies Corporation, Carlsbad, CA, USA) in 20 μl of reaction mix.

2.6 Qualitative PCR analysis

Qualitative PCR analysis was carried out using GoTaq® Flexi DNA polymerase (Promega Italia®, Milan, Italy). Total RNA was extracted from brain areas and tissues of 4 C57BL6/J mice and pooled before RT reaction. Primers were designed based on rat short IL-18Rβ (NCBI accession number: NM_184047) to produce two specific PCR products of 101 bp and 190 bp corresponding to the canonical and short IL-18b respectively (if a mouse analogue of the rat short IL-18Rβ exists): IL-18Rβ forward: AAG GCA TGC TGC ATA TAT TGG; IL-18Rβ reverse: TCT TGA TAC AAC AGG CCA TAT CC. Cyclophilin A mRNA (NCBI GenBank accession number: NM_008907) was used for normalization; the CypA forward: AGC ATA CAG GGT CCT GGC ATC and CypA reverse: TTC ACC TTC CCA AAG ACC AC. The PCR protocol was: 95°C for 2 min, 1 cycle; 95°C for 30 sec; 60°C for 30 sec; 72°C for 1 min, 35 cycles; 72°C for 10 min, 1 cycle. To verify that the sequence of the short IL-18Rβ did not correspond to any intermediate RNA form, we used a specific primer set whose forward (GTC CTC AAA TCA TCC CAG T) and reverse primer (CGG ACT GTC CAG GAA CTC AC) matched respectively with the intron 5 and the exon 7 of the mouse IL-18Rβ gene.

2.7 Amplification and DNA sequencing

To sequence the IL-18Rβ variants, we amplified the specific PCR products (of 101 bp and 190 bp) starting from cDNA equivalent to 0,9 mg total RNA (mouse cerebral cortex or spleen) using the same forward and reverse primers used for the qualitative distribution (see section 2.6 Methods) and GoTaq® Flexi DNA polymerase (Promega Italia®, Milan, Italy). To increase the amount of products needed for the sequence analysis we performed a modified NESTED PCR step using the same primer pairs on 1 ml of the first PCR product. The cycling parameters were: 95°C for 2 min, 1 cycle; 95°C for 30 sec, 58°C for 30 sec, 72°C for 1 min, 25 cycles; 72°C for 10 min, 1 cycle. Amplified PCR products were analyzed

by agarose gel electrophoresis and purified using Wizard® SV Gel and PCR Clean-Up System (Promega Italia®, Milan, Italy) following the manufacturer's instructions. 100 ng of both 101 bp and 190 bp PCR products from mouse cerebral cortex and spleen were sequenced from 5' and 3' ends on an ABI prism 377 DNA Sequencer using the ABI PRISM Big Dye Terminator chemistry (Perkin Elmer Biosystem®, Milan, Italy). The DNA sequences obtained were compared with published sequences in the GenBank database, by homology search using BLAST 2.0 (basic BLAST search, nr database, accessed at http://www.ncbi.nlm.nih.gov), and all sequences with significant homology were identified.

2.8 Real Time PCR

Real Time PCR was performed in ABI PRISM 7900 HT (Life Technologies Corporation, Carlsbad, CA, USA) using Power SYBR Green mix (Life Technologies Corporation, Carlsbad, CA, USA). To distinguish between the two splice variants of IL-18Rβ we designed a common forward primer complementary to nt 673–692 of the coding exon 5 and two specific reverse primers: full-length IL-18Rβ : GGG GGC TCC TAA TTC TGG G and short IL-18Rβ: GTC CTG TGA GCA CTT GTC TA. IL-18 (NCBI GenBank accession number: NM_008360) IL-1β (NCBI GenBank accession number: NM_008361), IL-18Rα type I (NCBI GenBank accession number: NM_008365), IL-18Rα type II (NCBI GenBank accession number: BC023240), and IL-18Rβ levels were normalized for each well to endogenous control cyclophilin A (CypA). The following forward and reverse sequences were used at the final concentration of 150 nM: IL-18 forward: TGA AGA AAA TGG AGA CCT GGA, IL-18 reverse: GGC TGT CTT TTG TCA ACG AAG; IL-1β forward: TGA AAG CTC TCC ACC TCA ATG, IL-1β reverse: CCA AGG CCA CAG GTA TTT TG; IL-18Rα type I forward: GAG TAA CTG TGC TTG TTC TCG CCT CTG T, IL-18Rα type I reverse: GGG TAA CGT CTC CAC ACG AAA AGT AT; IL-18Rα type II forward: GGC ACC CTA GCT CAT GTT TT; IL-18Rα type II reverse: AAC GAG GCT CAG AGA TCA TTA GT. The cycling parameters were: 95°C 10 min and 95 °C 15 s, 60° 1 min for 40 cycles. Single PCR products were subjected to a heat dissociation protocol (gradual increase of temperature from 60°C to 95 °C) and agarose gel separation to verify the absence of artifacts, such as primer-dimers or non-specific products. Direct detection of PCR products was monitored by measuring an increase in fluorescence intensity caused by binding of SYBR GREEN I dye to neo-formed double strand DNA during the amplification phase. Ct (cycle threshold) value was determined by the SDS software 2.2.2 (Life Technologies Corporation, Carlsbad, CA, USA) and was utilized to calculate mRNA fold changes using the delta delta ct (ΔΔCt) method. The equation used was $2^{\Delta\Delta ct} = 2^{(Ct_X - Ct_R)_{reference} - (Ct_X - Ct_R)_{target}}$, where Ct_X was the threshold cycle of the gene of interest (that were: IL-18 and the IL-18R chains) and Ct_R was the threshold cycle of the house-keeping gene (that was: cyclophilin A).

For an appropriate application of comparative ΔΔCt method, it was demonstrated that amplification efficiency of the target gene and endogenous control gene was approximately equal. Each cDNA sample was run in triplicate and the mean values were used to calculate the gene expression levels.

2.9 Statistical analysis

The relative quantity of short and full-length IL-18Rβ variants gene expression was analyzed by the ΔΔCt method using as calibrator average of the cerebral cortex of control (saline injected) animals. The mRNA levels of the targets genes were normalized on the intensity of the house-keeping gene, cyclophilin A. Cv values were obtained by an interpolate study. Regional brain differences in the expression of the canonical and the short IL-18Rβ variants were analyzed with a one factor analysis of variance (ONE-WAY ANOVA) followed by multiple post-hoc comparisons (Tukey HSD). Differences were considered significant if p< . 05. The effect of LPS on the expression pattern of the full- and short-length IL-18Rβ mRNA isoforms in the various brain areas were analyzed using a two-factor ANOVA. Individual planned post-hoc comparisons were performed (t-test) between LPS and saline treated animals for each individual brain area (p values below .05 were considered significant). The relative expression of full- and short-length IL-18Rβ in animals injected with LPS or vehicle (ratio) was analyzed using a two-factor ANOVA followed by planned post-hoc pair-wise comparisons. Differences were considered significant if $p < .05$. Finally the analysis of the effects of a peripheral LPS injection on the expression of the cytokine IL-18 and the two isoforms of the IL-18Rα (type I and II) was performed with a Student's t-test (comparative ΔΔCt method was performed using as calibrator average of saline control animals for each brain area; $p \leq .01$ was considered significant).

3. RESULTS

3.1 Identification of a mouse homologue of the short rat brain IL-18Rβ isoform

We demonstrated the existence of a short isoform of the mouse IL-18Rβ (sIL-18Rβ) which is supposedly similar to that described by Andre and coworkers (Andre et al., 2003). We used a forward primer matching the exon 5 and a reverse primer matching the exon 6 of mouse IL-18Rβ mRNA. In the presence of both beta chain isoforms these primers were expected to produce two specific products by RT-PCR. Qualitative PCR performed on mouse cDNA obtained from different brain areas as well as from spleen amplified two products of 101 bp and 190 bp for the canonical and the small IL-18Rβ isoform, respectively (Fig. 1). As demonstrated by sequencing, the latter PCR product includes a 89 bp fragment, downstream of the exon 5, previously known to be intronic (according to the homology with the published mouse sequence NCBI GenBank accession number: NM_010553).

The relative expression (abundance) of the canonical (full-length) and the short IL-18Rβ variants in the CNS were then evaluated using Real Time PCR. One-Way ANOVA revealed a statistically significative difference [$F(7,16) = 4.68$; $p = .005$] among the mean of the ΔΔct values (see Methods section) for the full-length 18Rβ mRNA expression in the different brain areas evaluated. Transcript levels of the full-length IL-18Rβ were highest in the olfactory bulb and in the frontal cortex followed by the striatum, the hypothalamus, the thalamus, the cerebellum and the cerebral cortex. The lowest relative levels of IL-18Rβ mRNA expression were found in the hippocampus (Fig. 2A). Post-hoc tests revealed a significant difference in full-length 18Rβ mRNA expression between the frontal cortex and the thalamus ($p = .007$). Moreover, the expression of the canonical IL-18Rβ mRNA was significantly higher in the olfactory bulb with respect to the striatum ($p = .034$), the

hypothalamus (p= .050), the thalamus (p= .000), the hippocampus (p= .005), the cerebellum (p= .034) and the cerebral cortex (p= .014). Furthermore, the levels of IL-18Rβ mRNA were relatively lower in all these brain regions when compared to the spleen (mean ± S.E.M.; 1480.08 ± 201.02) (data not shown).

With respect to the IL-18Rβ short isoform, a one-Way ANOVA revealed that the expression of this isoform doffers significantly among the brain areas considered [F(7,16) = 6.16; p = .001]. Similar to the full-length IL-18Rβ variant, the short IL-18Rβ mRNA variant was expressed at high levels in the olfactory bulb and in the frontal cortex and in the thalamus, with somewhat lower levels expressed in the cerebellum, the hippocampus, the hypothalamus, the striatum and the cerebral cortex (Fig. 2B). Post-hoc comparisons between areas revealed that the levels of the sIL-18Rβ mRNAs where higher in the olfactory bulbs compared to that of the striatum (p= .001), the hypothalamus (p= .002), the thalamus (p= .032), the hippocampus (p= .013), the cerebellum (p= .025) and the cerebral cortex (p= .001). Moreover, mRNA levels of the sIL-18Rβ were relatively lower in all these brain regions when compared to the spleen (2489.84 ± 756.81) (data not shown).

3.2 Basal expression and distribution of IL-18Rβ in the mouse brain

We next determined the anatomical distribution and localization of IL-18Rβ mRNA in the mouse brain. This was performed by *in situ* hybridization with digoxigenin-labeled cRNA anti-sense probes directed against a portion of the CDS (using a sense probe as a control) designed to detect the transcript for the canonical IL-18Rβ. An overall view of the distribution of the IL-18Rβ mRNA is presented in figure 3 and supplementary figure 2, while a comprehensive summary of its expression is presented in Table I.

In accordance with the PCR results (Fig. 2), high hybridization signal was observed in the telencephalon, in the orbitofrontal cortex (e.g. frontal association cortex-FrA and prelimbic cortex-PrL) (supplementary Fig. 2) and in the olfactory system (e.g. piriform cortex-Pir and anterior olfactory nuclei-AOD, AOL and AOV) (supplementary Fig. 2). Furthermore, a moderate IL-18Rβ mRNA signal was found in each layer (I to VI) of the cerebral cortex (Fig. 3) with a similar distribution pattern in the different cortical areas (data not shown). In the hippocampal formation the expression of the IL-18Rβ mRNA was mainly neuronal-like, with heavy IL-18Rβ mRNA staining in the pyramidal cell layer of the Ammon's horn (CA1-CA3) (Fig. 3). In the cerebral cortex and in the hippocampus, as observed also for other areas or nuclei, the staining was mainly confined to the cell body of the pyramidal neurons and was not found in their processes (Fig. 3). No, or very weak, staining was present in the stratum radiatum (Rad) and in the layers molecular (mol), lacunosum molecular (Lmol) and oriens (Or) of the hippocampus (Fig. 3). Moreover, a weak staining was observed in the granule cell layer (GrDG) and in the polymorph layer (PoDG) of the dentate gyrus (DG) (Fig. 3). Finally a moderate hybridization signal was observed in the indusium griseum (IG) and in the subiculum (S, including presubiculum - PrS and parasubiculum - PaS) of the hippocampal formation. While the IL-18Rβ mRNA staining in the basal ganglia was weak, a moderate to strong IL-18Rβ mRNA signal was detected in the amygdala (Fig. 3). Especially high levels of IL-18Rβ mRNA expression were found in the basolateral amygdaloid nucleus (anterior - BLA, and posterior - BLP, parts), in the posterior part of the basomedial

amygdaloid nucleus (BMP), and in the posteromedial cortical amygdaloid nucleus (PMCo). Strong IL-18Rβ mRNA staining was also observed in the septum especially in the nucleus of the vertical limb of the diagonal band (VDB). In the diencephalon high levels of IL-18Rβ mRNA expression were observed in the medial habenular nucleus (MhB), in the thalamus (particularly in the anterior thalamic nuclei such as the anteroventral thalamic nucleus - AV, the parataenial thalamic nucleus-PT and the anterior part of the paraventricular thalamic nucleus - PVA) and in the hypothalamus (with especially high levels in the paraventricular hypothalamic lateral magnocellular part - PaLM, in the paraventricular hypothalamic dorsal cap - PaDC and in the ventromedial hypothalamic nucleus dorsomedial part - VMHDM) (Fig. 3). Finally in the cerebellar cortex the cell body of the Purkinje cells showed a very dense staining for IL-18Rβ mRNA whereas the staining was very low in the molecular layer, confined only to a few cell bodies in the granular layer and almost absent in the white matter (Fig. 3).

3.3 Peripheral LPS treatment strongly elevated IL-18Rβ mRNA levels in the mouse brain

The LPS-induced regulation of IL-18Rβ mRNA expression in the mouse brain was assessed three hours after intraperitoneal injection of 100 μg (1μg/μl) of LPS or vehicle (saline-100 μl) followed by Real Time PCR on the same brain regions investigated for the basal level.

A two-factor ANOVA (LPS or saline injection × brain area) demonstrated an overall main effect of treatment [$F(15,32) = 331.17$; $p < .0001$] and brain area [$F(15,32) = 5.46$; $p < .0001$]. Moreover, an interaction was observed between the two terms [$F(15,32) = 3.10$, $p = .01$]. Three hours after LPS injection (100 μg/mouse), a marked increase in the expression of full-length IL-18Rβ was observed in all brain regions with respect to control levels detected in each distinct brain area (Fig. 4A) (in detail: frontal cortex: $t = 5.25$, $p = .006$; olfactory bulb: $t = 5.17$, $p = .007$; striatum: $t = 6.89$, $p = .002$; hypothalamus: $t = 8.01$, $p = .001$; thalamus: $t = 5.39$, $p = .006$; hippocampus: $t = 8.85$, $p = 9.01 \times 10^{-4}$; cerebral cortex: $t = 7.48$, $p = .002$; cerebellum: $t = 16.02$, $p = 8.86 \times 10^{-5}$).

The expression of the short IL-18Rβ variant was also strongly induced three hours after the LPS injection (100 mg/mouse) (Fig. 4B) but in a more pronounced way than observed for the full-length isoform. A two-factor ANOVA (type of injection × brain area) demonstrated an overall main effect of type of injection [$F(15,32) = 266.51$; $p < .0001$] and area [$F(15,32) = 3.48$; $p = .007$] whereas an interaction between the two terms was not observed. Significant LPS-induced up-regulation of the sIL-18b mRNA expression was observed in all areas evaluated (in detail: frontal cortex: $t = 6.64$, $p = .002$; olfactory bulb: $t = 6.27$, $p = .02$; striatum: $t = 102.08$, $p = 9.59 \times 10^{-5}$; hypothalamus: $t = 8.97$, $p = .012$; thalamus: $t = 4.56$, $p = .01$; hippocampus: $t = 5.08$, $p = .007$; cerebral cortex: $t = 12.31$, $p = 2.50 \times 10^{-4}$; cerebellum: $t = 9.00$, $p = 8.51 \times 10^{-4}$). As observed for the canonical beta chain, also the expression of the short variant of the accessory chain was not significantly changed following LPS injection in the spleen (data not shown).

In the spleen (used for comparison and for monitoring treatment efficacy), LPS treatment induced a tenfold increase in IL-1β mRNA expression ($t = 8.57$, $p = .001$) and a four hundred fold elevation of IL-6 mRNA ($t = 5.74$, $p = .004$). however, no effect was found

with respect to the expression levels of IL-18Rβ mRNA or, as previously reported by Abu Elhija and co-workers (2008), on IL-18Rα transcript (data not shown).

We also analyzed the relative expression of full- and short-length IL-18Rβ in animals injected with LPS or vehicle (supplementary Fig. 1). A two-factor ANOVA (LPS or saline injection × brain area) demonstrated an overall main effect of type of injection (LPS or vehicle) [$F(15,32) = 24.77$; $p < .0001$] and an interaction between the two terms [$F(15,32) = 2.47$; $p = .038$]. Planned post-hoc analyses revealed that relative differences in the expression of the full-length/short IL-18Rβ ratio in mice exposed to LPS or exposed to saline differed significantly only in the frontal cortex ($t = -3.33$, $p = .03$), in the olfactory bulb ($t = -3.521$, $p = .02$), and in the striatum ($t = -23.27$, $p < .001$). Ratios did not differ significantly in hypothalamus and cortex. This is possibly due to the high variance observed in these areas, which can in part be explained by the fact that in basal conditions the short IL-18Rβ variant was expressed at very low levels in these two areas (ct values were higher than 35).

Finally we evaluated the central effect of the same LPS challenge on other components of the IL-18 system including the cytokines IL-18 and the two isoforms of the alpha chain of the IL-18 receptor (supplementary Tab. 2).

Compared to saline injected animals, the peripheral administration of LPS significantly increased the levels of IL-18Rα type II specifically in the cerebral cortex ($t = 4.70$; $p = .009$) and in the hippocampus ($t = 4.48$; $p = .01$) whereas no significant ($p \geq .01$) effect was observed in the expression of IL-18Rα type I and IL-18 mRNAs in all brain areas evaluated (supplementary Tab. 2).

3.4. CNS basal and LPS-induced IL-18Rβ protein

Using immunohistochemistry, on paraffin-embedded brain sections, we have identified regions with endogenous basal expression of IL-18Rβ. We have highlighted the amigdala (Fig. 5A and 5B), cerebellum (Fig. 5C and 5D), hippocampus (Fig. 5E and 5F) and POA (Fig. 5G and 5H), In these regions as well as in others, LPS increased the expression of IL-18Rβ protein (Fig. 5B, D, F and H) in comparison to PBS-injected controls (Fig. 5A, C, E and G). Particularly in the cerebellum, we have noticed that the IL-18Rβ up-regulation occurred in neuronal cell bodies (Fig. 5C and 5D).

4. DISCUSSION

In situ hybridization demonstrated that in naive animals the transcript encoding for the canonical IL-18Rβ was expressed in the majority of the brain regions previously demonstrated to express IL-18Rα mRNA (Alboni et al., 2009). This suggested that neurons in these areas constitutively express functional IL-18R. Since such regions include the limbic system and other areas involved in emotion and motivational behaviour (Kötter and Meyer, 1992), IL-18 may have a role in the modulation of these functions. Remarkably, despite overall similar distribution, a few important differences were also found. In fact, the IL-18Rβ mRNA staining was: i) relatively low in the granular layer of the dentate gyrus (GrDG) of the hippocampus; ii) especially high in the amygdale; iii) lower in the preoptic

region compared to other hypothalamus regions. These differences may provide important clues for understanding the central action of IL-18. For instance, the differential distribution of receptor subunits in the hippocampus may explain why IL-18 was reported to attenuate long-term potentiation in the DG region (Cumiskey et al., 2007) while facilitating basal synaptic transmission in the CA1 (Kanno et al., 2004). Similarly, low IL-18Rβ in the preoptic area may be the reason for the observation that IL-18 lacked pirogenic action. Moreover, it is also possible that IL-18Rα could be able to form heterocomplexs with a receptor different from IL-18Rβ and *vice versa* for IL-18Rβ, suggesting that other cytokines (different to those tested by Cheung et al., 2005) may act via the β chain to activate intracellular pathways.

In the present report we also identify for the first time in the mouse brain a short IL-18Rβ splice variant similar to those previously described in rat and human tissues (including the brain) (Andre et al., 2003; Fiszer et al., 2007). In the mouse this short IL-18Rβ variant results from the insertion of a 89-bp fragment, previously known to be intronic, downstream of the exon 5. This insertion introduces a novel coding sequence that includes a stop codon. If the same ATG-star codon of the canonical IL-18Rβ is used this short variant mRNA is supposed to generate a 148 aa long peptide with the same 131 aa of the canonical IL-18Rβ N terminus and with a unique 17 aa long C-terminal tail. Similar to rat and human, the mouse short isoform is predicted to have the Ig-like C2-type 1 domain and to lack the transmembrane region suggesting it may represent a soluble form of the receptor. Although its biological function and significance remain to be demonstrated, it can be hypothesized that this isoform may negatively regulate IL-18 action. Since IL-18Rβ was not demonstrated to bind directly to IL-18, one possibility is that this short soluble form can compete with the canonical IL-18Rβ for the formation of a functional IL-18R heterodimer. Otherwise, the complexity of this system is further enhanced by the existence of a truncated IL-18Rα decoy (IL-18Rα type II) also demonstrated in the mouse CNS (Alboni et al., 2009). Similar to the soluble form of IL-1 receptor accessory protein, this short IL-18Rβ variant could inhibit IL-18 action by increasing the affinity of binding of IL-18 to IL-18Rα type II (Smith et al., 2003). The action of these isoforms may not be significant until stimulation occurs and might be region specific. In fact, we observed that, the short IL-18Rβ isoform was expressed at very low basal levels in unstimulated mouse brain but its relative abundance strongly increased after peripheral LPS administration in all the regions tested. Moreover, the levels of IL-18Rα type II, were also elevated by LPS specifically in the hippocampus and the cerebral cortex.

In addition to the IL-18Rβ transcriptional increment in LPS-injected animals in comparison to controls, the identification of enhanced protein levels visualized by immunohistochemistry supports a role for the IL-18 system in pathology, not only in inflammatory cells but also in neuronal cell types. In a Parkinson's disease mouse model, it has been suggested that microglia cells are involved in the IL-18-mediated neuronal loss (Sugama et al., 2004). However, given that cells with morphological characteristics of neurons do express IL-18Rα (Alboni et al., 2010) and IL-18Rβ, as reported here, in addition to the cytokine IL-18 (Sugama et al., 2002), it is possible that an up-regulation of these receptors in pathology causes direct damage to neuronal cell types.

Intraperitoneal injection of LPS induces the sickness syndrome, a condition characterized by physiological and behavioural symptoms commonly associated with infectious diseases. These include anorexia (Wisse et al., 2007), lethargy (Hopwood et al., 2009), memory impairments (Vereker E et al, 2000; Shaw KN et al., 2001), and a depressive-like state (Dantzer et al., 2008). These symptoms are associated with, and in part mediated by, LPS-dependent induction of pro-inflammatory cytokines, primarily IL-1β, TNF-α and IL-6 (Breder et al. 1994; Laye et al., 1994; Quan et al., 1999; Gatti and Bartfai, 1993). In addition, IL-18 was also proposed to contribute to this syndrome. Recent studies have shown that IL-18 is an anorexigenic agent and a regulator of energy efficiency (Netea et al., 2006, Zorrila et al., 2007), that induces sleep (Kubota et al., 2001), attenuates long term potentiating (Cumiskey et al., 2006) and regulates the HPA axis as well as the response to stressors (Sugama and Conti, 2008). The expression of IL-18 mRNA was not affected three hours after LPS exposure (100 mg/mouse) in all the brain areas evaluated. Given that here we demonstrate that IL-18 is expressed constitutively in the mouse brain as it is in the periphery (Fantuzzi et al., 2001; Puren et al., 1999), it is possible that in an early phase IL-18 may still influence neuronal processing via immune-challenge-dependent changes in receptor isoforms expression. For example, a similar mechanism has been suggested by Sareneva and coworkers (Sareneva et al., 2000) in T cells where IFN-a rapidly increases the IL-18R expression and sensitizes cells to lower concentration of IL-18 (in IL-18-induced NF-kB activity). It has also been demonstrated that *in vivo* brain levels of mature IL-18 were elevated one week after peripheral LPS injection (Yaguchi et al., 2009), so we cannot exclude that at later time LPS-induced response could trigger IL-18 expression. Notably, the expression of short variant of the IL-18Rβ was more induced that than of the canonical IL-18Rβ variants and the full-length/short IL-18Rβ isoforms ratio particularly affected in specific brain area (i.e.frontal cortex, olfactory bulb, and striatum).

The main feature of our approach is that it better highlights the differences in the regulation of the IL-18 system in different brain areas. However, future studies will be needed to better understand the kinetics of the regulation of this system in the light of its role in the CNS.

Summarizing, LPS strongly IL-18Rβ variants expression and change the ration between this two proteins in the brain (these effect were not found in the spleen) and this should be considered when trying to understand the biology of central IL-18 action. It may be interesting in the future to understand to what extent these mechanisms regulate the activation and/or the termination of IL-18 signaling.

Overall we provide evidence suggesting that central regulation of the levels of IL-18 receptor subunits and isoforms may modulate IL-18 action in the brain. Yet, the possibility that IL-18Rα ligands, other than IL-18, may exist cannot be excluded (Gutcher et al., 2006).

Summarizing we can observe that, like the IL-18Rα mRNA, the IL-18Rβ mRNA is mainly expressed in those areas that are, or have been considered to be, parts of the limbic system (i.e. hippocampus and amygdala but also the obitrofrontal cortex, piriform cortex and olfactory bulb) or that are connected with this system (i.e. habenula). Since this system supports several functions including memory, emotion, motivational behaviour and olfaction

(Kötter and Meyer, 1992), we may suppose that IL-18 could participate in the regulation of these functions by modifying cell activity in the brain through the activation of its receptor.

Supplementary Material

Refer to Web version on PubMed Central for supplementary material.

ACKNOWLEDGMENTS

Dr. Silvia Alboni research was partially funded by a fellowship for young scientists in foreign countries from the Italian Society of Pharmacology (SIF). Partially supported by HL088083

ABBREVIATIONS

3V	third ventricle
7	facial nucleus
AAD	anterior amygdaloid area dorsal part
AAV	anterior amygdaloid area ventral part
Acb	nucleus accumbens
ACo	cortical amygdaloid nucleus anterior part
AD	anterodorsal thalamic nuclei
AHA	anterior hypothalamic area anterior part
AHC	anterior hypothalamic area central part
AHiAL	amygdalohippocampal area anterolateral part
AHiPM	amygdalohippocampal area postmedial part
AHP	anterior hypothalamic area posterior part
AI	agranular insular cortex
Aint	anterior interposed nucleus
AIP	agranular insular cortex posterior part
AM	anteromedial thalamic nuclei
AOD	anterior olfactory nucleus dorsal part
AOL	anterior olfactory nucleus lateral part
AOM	anterior olfactory nucleus medial part
AOV	anterior olfactory nucleus ventral part
APir	amygdalopiriform transition area

APT	anterior pretectal nucleus
Arc	arcuate hypothalamic nucleus
Au1	primary auditory cortex
AuD	auditory cortex dorsal part
AuV	auditory cortex ventral part
AV	anteroventral thalamic nuclei
AVPe	anteroventral periventricular nucleus
BAOT	bed nucleus of accessory olfactory tract
BLA	basolateral amygdaloid nucleus anterior part
BLP	basolateral amygdaloid nucleus posterior part
BLV	basolateral amygdaloid nucleus ventral part
BMA	basomedial amygdaloid nucleus anterior part
BMP	basomedial amygdaloid nucleus posterior part
BST	bed nucleus of stria terminalis
CA	Ammon’s horn
CA1	CA1 field of the hippocampus
CA2	CA2 field of the hippocampus
CA3	CA3 field of the hippocampus
CeC	central amygdaloid nucleus capsular division
CeL	central amygdaloid nucleus lateral division
CeM	central amygdaloid nucleus medial division
Cg1	cingulate cortex area 1
Cg2	cingulate cortex area 2
Circ	circular nucleus
CPu	caudate-putamen (striatum)
DC	dorsal cochlear nucleus
DEn	dorsal endopiriform nucleus
DG	dentate gyrus
DLG	dorsal lateral genicolate nucleus

DLO	dorsolateral orbital cortex
DM	dorsomedial hypothalamic nucleus
DMC	dorsomedial hypothalamic nucleus compact part
DMD	dorsomedial hypothalamic nucleus diffuse part
DMV	dorsomedial hypothalamic nucleus ventral part
DP	dorsal peduncular cortex
DpG	deep gray layer of the superior colliculus
DpMe	deep mesencephalic nucleus
DR	dorsal raphe nucleus
DTM	dorsal tuberomammillary nucleus
DTT	dorsal tenia tecta
Ect	ectorhinal cortex
EPI	external plexiform layer of the olfactory bulb
EW	Edinger-Westphal nucleus
FrA	frontal association cortex
Gi	gigantocellular reticular nucleus
GI	granular insular cortex
Gl	glomerular layer of the olfactory bulb
GrDG	granular layer of the dentate gyrus
GrL	granular cell layer of the cerebellar cortex
GrO	granule layer of the olfactory bulb
HDB	nucleus of the horizontal limb of the diagonal band
IG	indusium griseum
IL	infralimbic cortex
IMLF	interstitial nucleus of the medial longitudinal fasciculus
InG	intermediate gray layer of the superior colliculus
IPl	internal plexiform layer of the olfactory bulb
La	lateral amygdaloid nucleus
LA	lateroanterior hypothalamic nucleus

Lat	lateral (dentate) cerebellar nucleus
LEnt	lateral entorhinal cortex
LH	lateral hypothalamic area
LHb	lateral habenular nucleus
LM	lateral mammillary nucleus
LMol	lacunosum molecular layer of the hippocampus
LO	lateral orbital cortex
LOT	nucleus of lateral olfactory tract
LPO	lateral preoptic area
LSD	lateral septal nucleus dorsal part
LSI	lateral septal nucleus intermediate part
LSV	lateral septal nucleus ventral part
M1	primary motor cortex
M2	secondary motor cortex
MCLH	magnocellular nucleus of the lateral hypothalamic area
MCPO	magnocellular preoptic nucleus
MD	mediodorsal thalamic nucleus
Me	medial amygdaloid nucleus
ME	median eminence
Med	medial (fastgial) cerebellar nucleus
MHb	medial habenular nucleus
Mi	mitral cell layer of the olfactory bulb
ML	medial mammillary nucleus lateral part
MM	medial mammillary nucleus
MnPO	median preoptic nucleus
MnR	median raphe nucleus
MO	medial orbital cortex
Mol	molecular layer of the dentate gyrus
MOL	molecular layer of the cerebellar cortex

MPA	medial preoptic area
MPOC	medial preoptic nucleus central part
MPOL	medial preoptic nucleus lateral part
MPOM	medial preoptic nucleus medial part
MS	medial septal nucleus
MVe	medial vestibular nucleus
Or	oriens layer hippocampus
P	Purkinje cell layer
PAG	periaqueductal gray
PaDC	paraventricular hypothalamic dorsal cap
PaLM	paraventricular hypothalamic lateral magnocellular part
PaMM	paraventricular hypothalamic medial magnocellular part
PaMP	paraventricular hypothalamic medial parvicellular part
PaPO	paraventricular hypothalamic nucleus posterior
PaS	parasubiculum
PaV	paraventricular hypothalamic nucleus ventral part
Pe	periventricular hypothalamic nucleus
PF	parafascicular thalamic nucleus
PH	posterior hypothalamic area
Pir	piriform cortex
PLCo	posterolateral cortical amygdaloid nucleus
PMCo	posteromedial cortical amygdaloid nucleus
PMD	premammillary nucleus dorsal
PMV	premammillary nucleus ventral part
POA	preoptic area
PoDG	polymorph layer dentate gyrus
PPtA	posterior parietal association area
PRh	perirhinal cortex
PrL	prelimbic cortex

PrS	presubicilum
PS	parastrial nucleus
PT	parataenial thalamic nucleus
PV	paraventricular thalamic nucleus
PVA	paraventricular thalamic nucleus anterior part
Py	pyramidal cell layer of the hippocampus
Rad	stratum radiatum of the hippocampus
RCh	retrochiasmatic area
Re	reuniens thalamic nuclei
RLi	rostral linear nucleus raphe
RMC	red nucleus magnocellular
RMg	raphe magnus nucleus
RPC	red nucleus parvocellular
RSA	retrosplenial agranular cortex
RSG	retrosplenial granular cortex
Rt	reticular thalamic nucleus
S	subiculum
S1	primary somatosensory cortex
S2	secondary somatosensory cortex
SchDM	suprachiasmatic nucleus dorsomedial part
SchVL	suprachiasmatic nucleus ventrolateral part
SI	substantia innominata
SLu	stratum lucidem of the hippocampus
SMT	submammillothalamic nucleus
SNC	substantia nigra compact part
SNL	substantia nigra lateral part
SNR	substantia nigra reticular part
SO	supraoptic nucleus
Sp5ODM	spinal 5 nucleus oral dorsomedial part

Sp5OVL	spinal 5 nucleus oral ventrolateral part
STh	subthalamic nucleus
SuG	superficial gray superior colliculus
SuM	supramammillary nucleus
SuMM	supramammillary nucleus, medial part
SuVe	superior vestibular nucleus
TC	tuber cinereum area
TS	triangular septal nucleus
Tu	olfactory tubercle
V1B	primary visual cortex binocular region
V1M	primary visual cortex monocular region
V2L	secondary visual cortex lateral part
V2ML	secondary visual cortex mediolateral part
V2MM	secondary visual cortex mediomedial part
VCP	ventral cochlear nucleus posterior part
VDB	nucleus of the vertical limb of the diagonal band
VL	ventrolateral thalamic nucleus
VLG	ventrolateral genicolate nucleus
VLPO	ventrolateral preoptic nucleus
VM	ventromedial thalamic nucleus
VMH	ventromedial hypothalamic nucleus
VMHC	ventromedial hypothalamic nucleus central part
VMHDM	ventromedial hypothalamic nucleus dorsomedial part
VMHVL	ventromedial hypothalamic nucleus ventrolateral part
VMPO	ventromedial preoptic nucleus
VO	ventral orbital cortex
VOLT	vascular organ of the lamina terminalis
VP	ventral pallidum
VPL	ventral posterolateral thalamic nucleus

VPM	ventral posteromedial thalamic nucleus
VTA	ventral tegmental area
VTM	ventral tuberomammillary nucleus
W	white matter
ZI	zona incerta

REFERENCES

Abu EM, Lunenfeld E, Huleihel M, 2008 LPS increases the expression levels of IL-18, ICE and IL-18 R in mouse testes. Am J Reprod Immunol. 60(4), 361–371. [PubMed: 19046143]

Alboni S, Cervia D, Ross B, Montanari C, Gonzalez AS, Sanchez-Alavez M, Marcondes MC, De Vries D, Sugama S, Brunello N, Blom J, Tascedda F, Conti B 2009 Mapping of the full length and the truncated interleukin-18 receptor alpha in the mouse brain. J Neuroimmunol. 214, 43–54. [PubMed: 19640592]

Alboni S, Cervia D, Sugama S, Conti B 2010 Interleukin 18 in the CNS. J Neuroinflammation. 29, 7–9.

Andre R, Wheeler RD, Collins PD, Luheshi GN, Pickering-Brown S, Kimber I, Rothwell NJ, Pinteaux E 2003 Identification of a truncated IL-18R beta mRNA: a putative regulator of IL-18 expressed in rat brain. J Neuroimmunol. 145(1–2), 40–45. [PubMed: 14644029]

Born TL, Thomassen E, Bird TA, Sims JE 1998 Cloning of a novel receptor subunit, AcPL, required for interleukin-18 signaling. J Biol Chem. 273, 29445–29450. [PubMed: 9792649]

Breder CD, Hazuka C, Ghayur T, Klug C, Huginin M, Yasuda K, Teng M, Saper CB 1994 Regional induction of tumor necrosis factor alpha expression in the mouse brain after systemic lipopolysaccharide administration. Proc Natl Acad Sci U S A. 91(24), 11393–11397. [PubMed: 7972071]

Cheung H, Chen NJ, Cao Z, Ono N, Ohashi PS, Yeh WC 2005 Accessory protein-like is essential for IL-18-mediated signaling. J Immunol. 174, 5351–5357. [PubMed: 15843532]

Cumiskey D, Pickering M, O'Connor JJ, 2007 Interleukin-18 mediated inhibition of LTP in the rat dentate gyrus is attenuated in the presence of mGluR antagonists. Neurosci Lett. 412(3), 206–210. [PubMed: 17123727]

Dantzer R, Bluthé RM, Layé S, Bret-Dibat JL, Parnet P, Kelley KW, 1998 Cytokines and sickness behavior. Ann N Y Acad Sci. 840, 586–590. [PubMed: 9629285]

Dantzer R, O'Connor JC, Freund GG, Johnson RW, Kelley KW, 2008 From inflammation to sickness and depression: when the immune system subjugates the brain. Nat Rev Neurosci. 9(1), 46–56. [PubMed: 18073775]

Fantuzzi G, Reed D, Qi M, Scully S, Dinarello CA, Senaldi G, 2001 Role of interferon regulatory factor-1 in the regulation of IL-18 production and activity. Eur J Immunol. 31, 369–75. [PubMed: 11180100]

Fiszer D, Rozwadowska N, Rychlewski L, Kosicki W, Kurpisz M 2007 Identification of IL-18RAP mRNA truncated splice variants in human testis and the other human tissues. Cytokine. 39(3), 178–183. [PubMed: 17897836]

Franklin KBJ, Paxinos G, 1997 The mouse brain in stereotaxic cooredinates, San Diego, Academic Press.

Frenois F, Moreau M, O'Connor J, Lawson M, Micon C, Lestage J, Kelley KW, Dantzer R, Castanon N, 2007 Lipopolysaccharide induces delayed FosB/DeltaFosB immunostaining within the mouse extended amygdala, hippocampus and hypothalamus, that parallel the expression of depressive-like behavior. Psychoneuroendocrinology. 32(5), 516–531. [PubMed: 17482371]

Gatti S, Bartfai T, 1993 Induction of tumor necrosis factor-alpha mRNA in the brain after peripheral endotoxin treatment: comparison with interleukin-1 family and interleukin-6. Brain Res. 624(1–2), 291–294. [PubMed: 8252403]

Gutcher I, Urich E, Wolter K, Prinz M, Becher B, 2006 Interleukin 18-independent engagement of interleukin 18 receptor-alpha is required for autoimmune inflammation. Nat Immunol. 7(9), 946–953. [PubMed: 16906165]

Hopwood N, Maswanganyi T, Harden LM, 2009 Comparison of anorexia, lethargy, and fever induced by bacterial and viral mimetics in rats. Can J Physiol Pharmacol. 87(3), 211–220. [PubMed: 19295662]

Hoshino K, Tsutsui H, Kawai T, Takeda K, Nakanishi K, Takeda Y, Akira S 1999 Cutting edge: generation of IL-18 receptor-deficient mice: evidence for IL-1 receptor-related protein as an essential IL-18 binding receptor. J Immunol. 162, 5041–5044. [PubMed: 10227969]

Kanno T, Nagata T, Yamamoto S, Okamura H, Nishizaki T, 2004 Interleukin-18 stimulates synaptically released glutamate and enhances postsynaptic AMPA receptor responses in the CA1 region of mouse hippocampal slices. Brain Res. 1012, 190–193. [PubMed: 15158178]

Kötter R, Meyer N, 1992 The limbic system: a review of its empirical foundation. Behav Brain Res. 52(2), 105–127. [PubMed: 1294190]

Kubota T, Fang J, Brown RA, Krueger JM, 2001 Interleukin-18 promotes sleep in rabbits and rats. Am J Physiol Regul Integr Comp Physiol. 281, R828–R838. [PubMed: 11506998]

Layé S, Parnet P, Goujon E, Dantzer R, 1994 Peripheral administration of lipopolysaccharide induces the expression of cytokine transcripts in the brain and pituitary of mice. Brain Res Mol Brain Res. 27, 157–62. [PubMed: 7877446]

Meyer TA, Noguchi Y, Ogle CK, Tiao G, Wang JJ, Fischer JE, Hasselgren PO, 1994 Endotoxin stimulates interleukin-6 production in intestinal epithelial cells. A synergistic effect with prostaglandin E2. Arch Surg. 129(12), 1290–1295. [PubMed: 7986158]

Netea MG, Joosten LA, Lewis E, Jensen DR, Voshol PJ, Kullberg BJ, Tack CJ, van Krieken H, Kim SH, Stalenhoef AF, van de Loo FA, Verschueren I, Pulawa L, Akira S, Eckel RH, Dinarello CA, van den Berg W, van der Meer JW, 2006 Deficiency of interleukin-18 in mice leads to hyperphagia, obesity and insulin resistance. Nat Med. 12, 650–656. [PubMed: 16732281]

Puren AJ, Fantuzzi G, Dinarello CA, 1999 Gene expression, synthesis, and secretion of interleukin 18 and interleukin 1beta are differentially regulated in human blood mononuclear cells and mouse spleen cells. Proc Natl Acad Sci U S A. 96, 2256–61. [PubMed: 10051628]

Okamura H, Kashiwamura S, Tsutsui H, Yoshimoto T, Nakanishi K 1998 Regulation of interferon-gamma production by IL-12 and IL-18. Curr Opin Immunol. 10, 259–264. [PubMed: 9638361]

Quan N, Stern EL, Whiteside MB, Herkenham M, 1999 Induction of pro-inflammatory cytokine mRNAs in the brain after peripheral injection of subseptic doses of lipopolysaccharide in the rat. J Neuroimmunol. 93, 72–80. [PubMed: 10378870]

Sareneva T, Julkunen I, Matikainen S, 2000 IFN-alpha and IL-12 induce IL-18 receptor gene expression in human NK and T cells. J Immunol. 165, 1933–8. [PubMed: 10925275]

Sergi B, Penttila I, 2004 Interleukin 18 receptor. J Biol Regul Homeost Agents. 18, 55–61. [PubMed: 15323361]

Shaw KN, Commins S, O'Mara SM, 2001 Lipopolysaccharide causes deficits in spatial learning in the watermaze but not in BDNF expression in the rat dentate gyrus. Behav Brain Res. 124(1), 47–54. [PubMed: 11423165]

Smith DE, Hanna R, Della Friend, Moore H, Chen H, Farese AM, MacVittie TJ, Virca GD, Sims JE 2003 The soluble form of IL-1 receptor accessory protein enhances the ability of soluble type II IL-1 receptor to inhibit IL-1 action. Immunity. 18(1), 87–96. [PubMed: 12530978]

Sugama S, Cho BP, Baker H, Joh TH, Lucero J, Conti B 2002 Neurons of the superior nucleus of the medial habenula and ependima cells express IL-18 in rat CNS. Brain Res. 958, 1–9. [PubMed: 12468024]

Sugama S, Wirz SA, Barr AM, Conti B, Bartfai T, Shibasaki T, 2004 Interleukin-18 null mice show diminished microglial activation and reduced dopaminergic neuron loss following acute 1-methyl-4-phenyl-1,2,3,6-tetrahydropyridine treatment. Neuroscience. 128, 451–458. [PubMed: 15350655]

Sugama S, Conti B, 2008 Interleukin-18 and stress. Brain Res Rev. 58, 85–95. [PubMed: 18295340]

Takeda K, Tsutsui H, Yoshimoto T, Adachi O, Yoshida N, Kishimoto T, Okamura H, Nakanishi K, Akira S 1998 Defective NK cell activity and Th1 response in IL-18-deficient mice. Immunity. 8, 383–390. [PubMed: 9529155]

Torigoe K, Ushio S, Okura T, Kobayashi S, Taniai M, Kunikata T, Murakami T, Sanou O, Kojima H, Fujii M, Ohta T, Ikeda M, Ikegami H, Kurimoto M 1997 Purification and characterization of the human interleukin-18 receptor. J Biol Chem. 272, 25737–25742. [PubMed: 9325300]

Vereker E, Campbell V, Roche E, McEntee E, Lynch MA, 2000 Lipopolysaccharide inhibits long term potentiation in the rat dentate gyrus by activating caspase-1. J Biol Chem. 275(34), 26252–26258. [PubMed: 10856294]

Wisse BE, Ogimoto K, Tang J, Harris MK Jr., Raines EW, Schwartz MW, 2007 Evidence that lipopolysaccharide-induced anorexia depends upon central, rather than peripheral, inflammatory signals. Endocrinology. 148(11), 5230–5237. [PubMed: 17673516]

Yaguchi T, Nagata T, Yang D, Nishizaki T, 2010 Interleukin-18 regulates motor activity, anxiety and spatial learning without affecting synaptic plasticity. Behav Brain Res. 206(1), 47–51. [PubMed: 19729040]

Zorrila EP, Sanchez-Alavez M, Sugama S, Brennan M, Fernandez R, Bartfai T, Conti B, 2007 Interleukin-18 controls energy homeostasis by suppressing appetite and feed efficiency. Proc Natl Acad Sci U S A. 104, 11097–11102. [PubMed: 17578927]

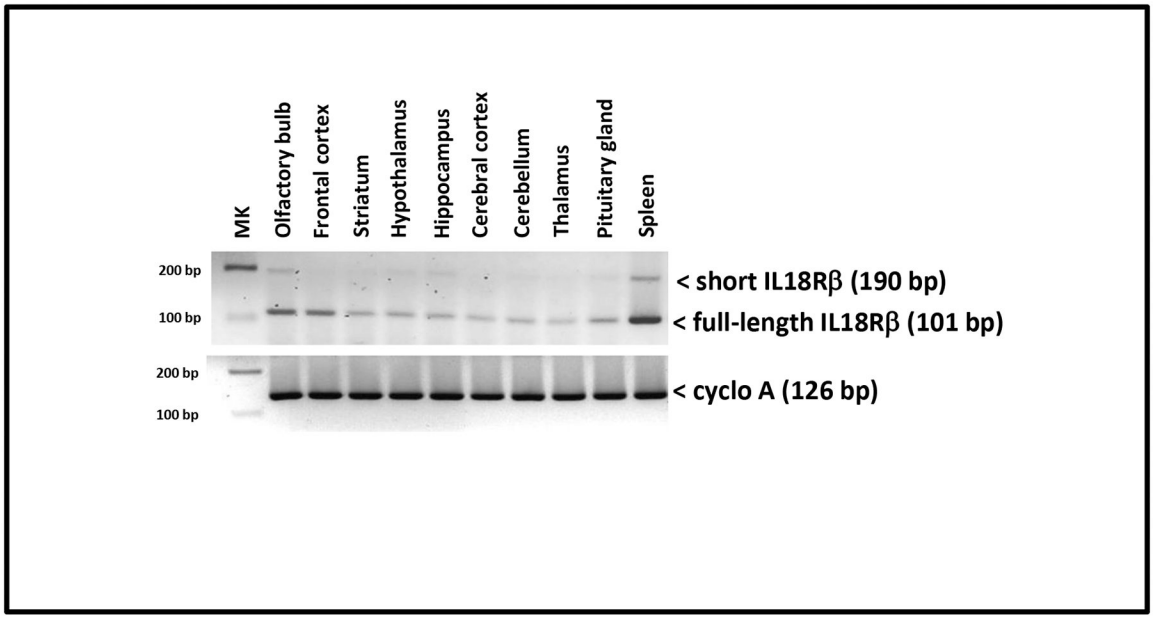

Figure 1: qualitative expression of the canonical (full-length) and short beta chain of the IL-18R in the mouse CNS and spleen.

We designed on IL-18Rβ mRNA (NCBI GenBank accession number: NM_010553) a forward primer matching the exon 5 and a reverse primer on the exon 6 of the transcript (see 2.6 Methods for sequence details). These primers amplified two products corresponding to the full-length IL-18Rβ at 101bp and to the short IL-18Rβ at 190bp. The latter results from the presence of the 89-bp long fragment previously believed to be an intronic sequence between exons 5 and 6. The absence of genomic contamination was also evaluated. We used a primer pair for Cyclophilin A as internal control.

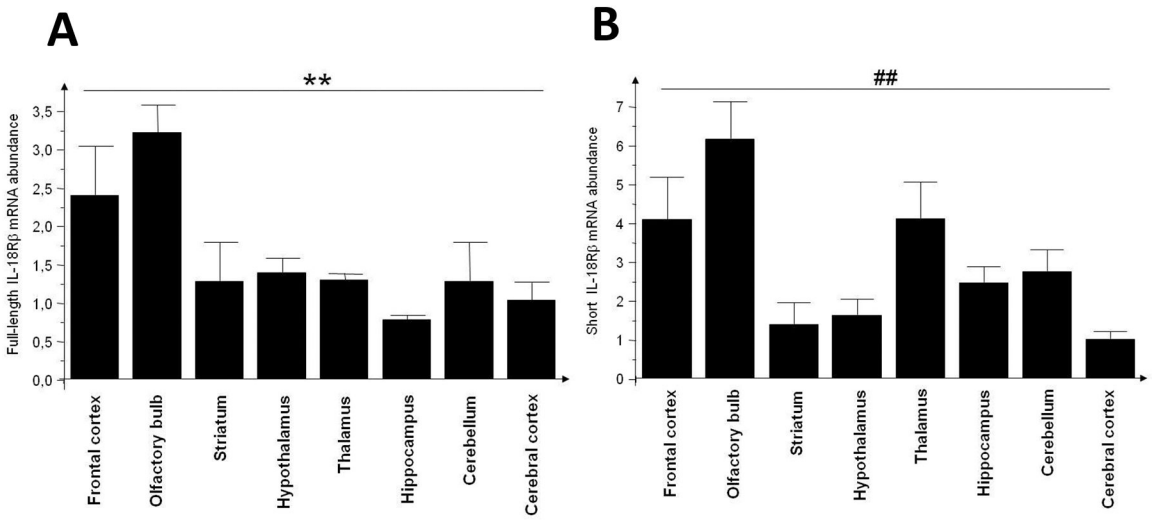

Figure 2: Histogram showing the relative level of the canonical (full-length) (A) and short (B) beta chain determined by quantitative PCR.

Levels of IL-18Rβ transcripts in each brain area were normalized with those of Cyclophilin A. The normalized level in the cerebral cortex was arbitrarily assigned the value of 1.00. *Each* column represents mean ± S.E.M.; ** $p = .005$ and $^{\#\#}$ $p = .001$ among the brain areas for the canonical or short IL-18Rβ variants respectively (One-Way ANOVA).

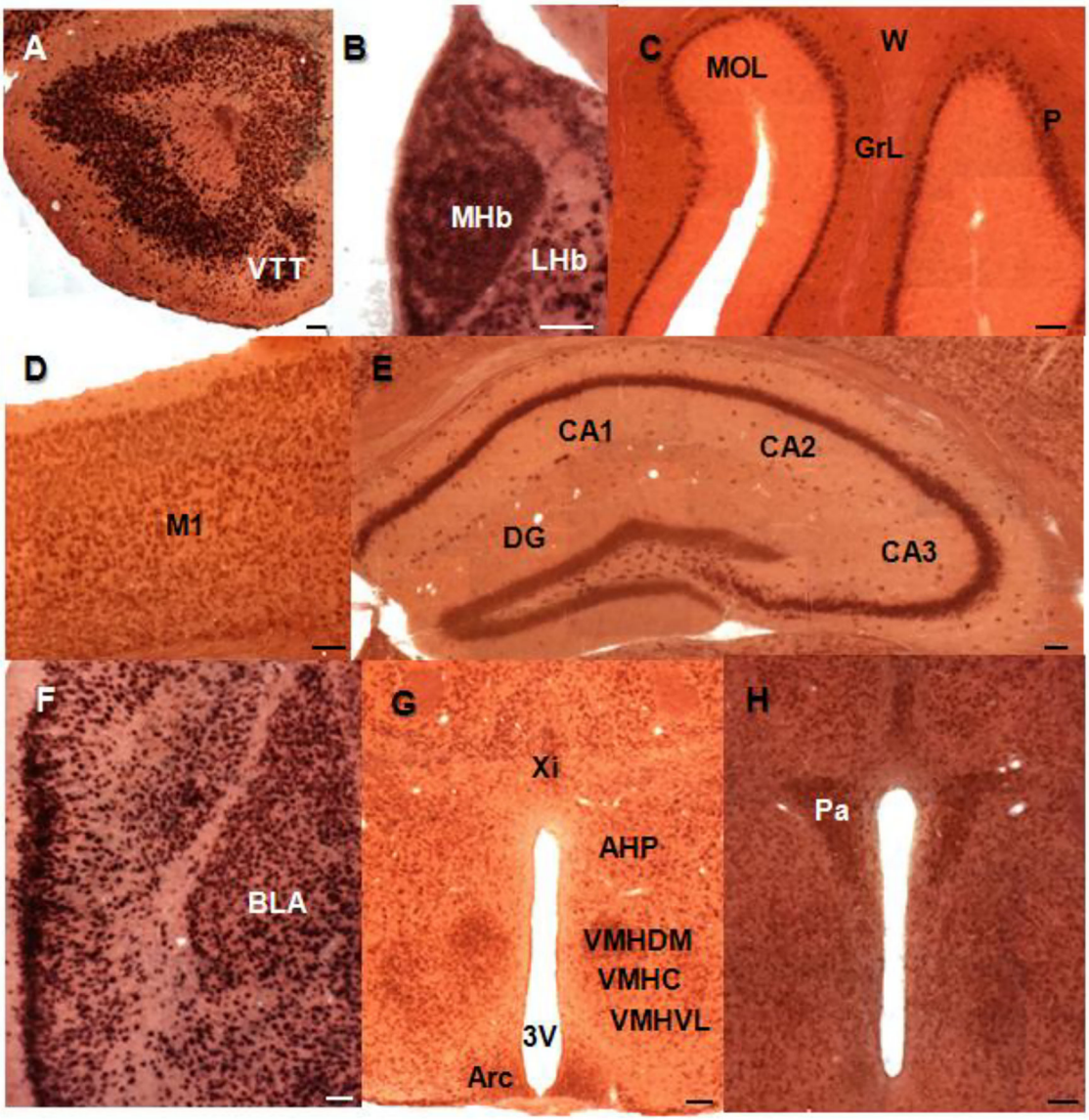

Figure 3: particulars of the localization of the IL-18Rβ mRNA hybridization signal in the CNS of C57BL6/J mice.

Note the positive nuclei stained dark brown. (A) the olfactory bulb (VTT-ventral taenia tecta); (B) the habenula (MHb-medial habenular nuclei, LHb-lateral habenular nuclei); (C) the cerebellar cortex (P-Purkinje cell layer, MOL-molecular layer, GrL-granular layer, W-white matter); (D) the cerebral cortex (M1-primary motor cortex); (E) the hippocampal formation (DG-dentate gyrus, CA1-CA1 field of the hippocampus, CA2-CA2 field of the hippocampus, CA3-CA3 field of the hippocampus); (F) the amygdala (BLA-basolateral amygdaloid nucleus anterior part); (G-H) the hypothalamus (Arc-arcuate hypothalamic nucleus, AHP-anterior hypothalamic area posterior part, VMHDM-ventromedial hypothalamic nucleus dorsomedial part, VMHC ventromedial hypothalamic nucleus central part, VMHVL-ventromedial hypothalamic nucleus ventrolateral part, Xi-xiphoid thalamic nucleus, , 3V-3th ventricle, Pa-paraventricular hypothalamic nucleus). Scale bar = 100μm.

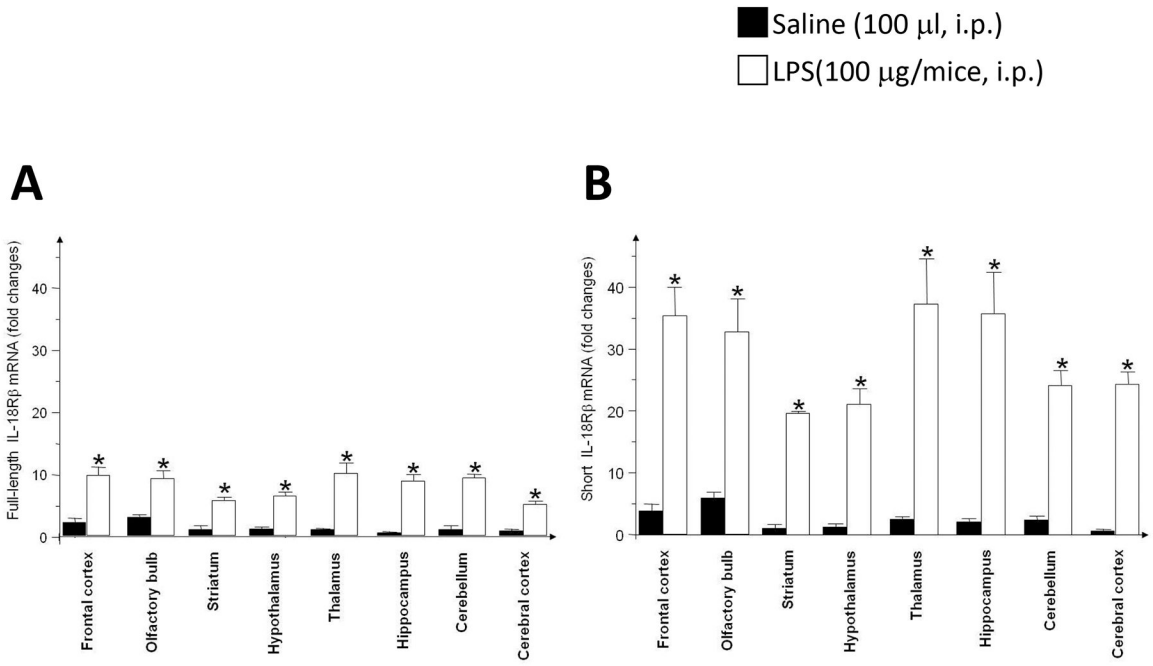

Figure 4: LPS (100 µg/mouse i.p.) strongly induces the expression of the full-length (A) and short (B) IL-18Rβ in the C57BL6/J mouse brain.

Adult mice were injected i.p. with LPS (100 µg/mouse, n=3) (white bars) or saline (100 µl/mice n=3) (black bars) and then sacrificed 3 hrs after injection. The relative expression levels of IL-18Rβ mRNA variants in brain areas: frontal cortex, olfactory bulb, striatum, hypothalamus, thalamus, hippocampus, cerebral cortex and cerebellum, were evaluated by real time PCR using specific primers. Data were expressed as fold-change above the expression of the respective cerebral cortex of control (saline injected) animals (see Methods for equation used). Bars indicate the mean ± S.E.M. * Statistical significant difference between LPS injected and control (saline injected) animals. *$p < .05$.

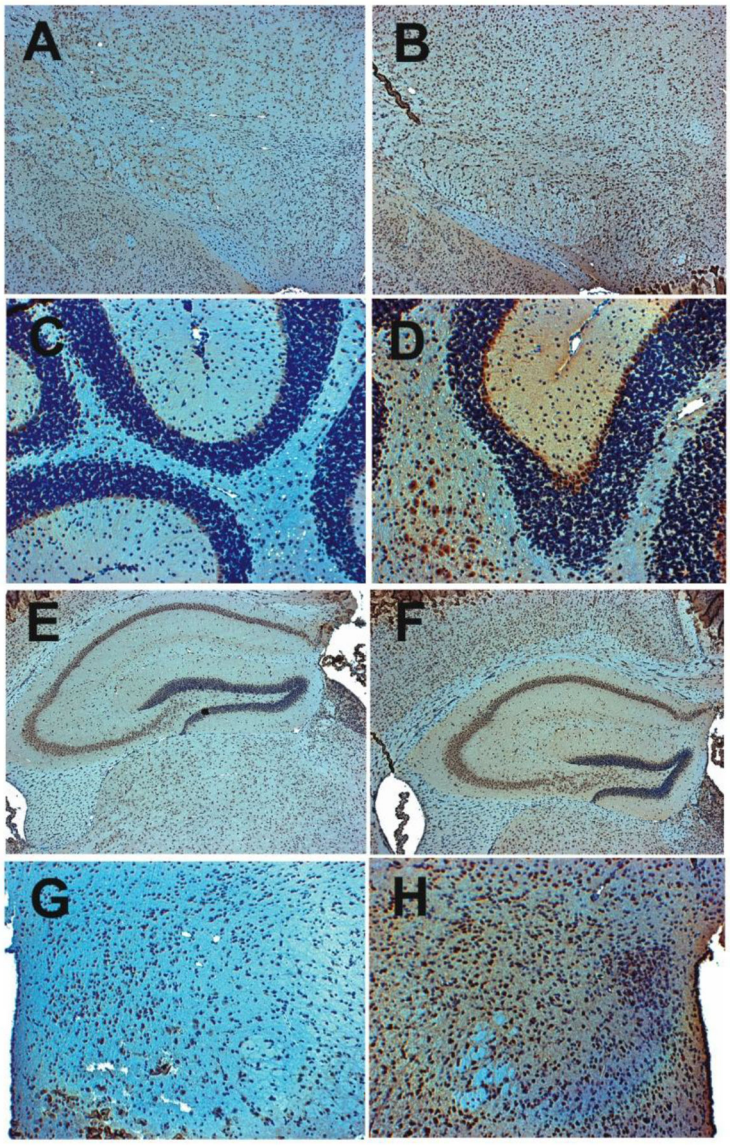

Figure 5: Immunohistochemical localization of the IL-18Rβ protein in the mouse brain under basal conditions and following LPS injection.

A, C, E and G show a representative animal that was injected with PBS. B, D, F and H show a representative animal that was injected with LPS. (A) and (B) represent the amigdala, (40×); (C) and (D) represent the cerebellum (64×); (E) and (F) represent the hipoccampus (40×) and (G) and (H) represent the POA (64×). LPS enhanced the expression of the IL-18Rβ molecule on neurons, in particular at the cell body level.

Table 1 –

expression of IL-18Rβ in the adult mouse brain

Area/nucleus	**IL-18Rβ**
Telencephalon	
Cerebral Cortex	
Orbitofrontal cortex	
FrA	++(+++)
DLO	++(+++)
MO	++(+++)
LO	++(+++)
VO	++
PrL	++(+++)
Motor cortex	
Ml	++
M2	++
Cingulate cortex	
Cg1	++
Cg2	++
RSG	++
RSA	++
Insular cortex	
GI	++
AI	++
AIP	++
IL	++
DP	++
Somatosensory cortex	
S1	++
S2	++

Brain Behav Immun. Author manuscript; available in PMC 2019 October 23.

Area/nucleus	IL-18Rβ
Auditory cortex	
Au1	++
AuD	++
AuV	++
Rhinal cortex	
Ect	+/++
PRh	+/++
LEnt	+/++
Visual cortex	
V1M; V1B	++
V2L; V2ML	++
V2MM	++
PPtA	++
Olfactory system	
GI	
EPI	
Mi	
IPI	
GrO	+
AOD	++(+++)
AOL	++(+++)
AOM	++
AOV	++(+++)
DTT	+(++)
Tu	+(++)
Pir	++(+++)
DEn	+(++)
Hippocampal formation	
IG	++

Area/nucleus	IL-18Rβ
CA1; CA2; CA3	
Or	+/–
Py	+++
LMol	
SLu	+/–
Rad	+/–
DG	
GrDG	+
Mol	
PoDG	+
S	
PrS; PaS	++
Basal ganglia	
Acb	+/–
Cpu	+
VP	+
Amygdala	
AAD	+/++
AAV	+/++
APir	++
LOT	++
BST	++
BAOT	+++
AHiAL	++
AHiPM	++
ACo	+
PLCo	+(++)
PMCo	++(+++)
CeC; CeL; CeM	+(++)

Area/nucleus	IL-18Rβ
BLA	++(+++)
BLP	++(+++)
BLV	+(++)
BMA	+(++)
BMP	++(+++)
La	++
Me	+(++)
Septum	
LSD	++
LSI	+(++)
LSV	+(++)
MS	++
VDB	++(+++)
HDB	++
TS	+
Diencephalon	
Epithalamus, thalamus and subthalamus	
MHb	++(+++)
LHb	++
Rt	++
PF	+(++)
Re	++
Anterior thalamic nuclei	
AD	++
AV	++(+++)
AM	++
PV	+(++)
PVA	++(+++)

Area/nucleus	IL-18Rβ
MD	++
PT	++(+++)
Lateral thalamic nuclei	
VL	+(++)
VM	+(++)
VPL	++
VPM	++
Posterior thalamic nuclei	
DLG	+(++)
VLG	+(++)
SI	+
ZI	+
STh	++
Hypothalamus	
Preoptic region	
LPO	+
MCPO	+(++)
SO	++
PS	+
MPA	+(++)
MPOC	++
MPOM	++
MPOL	++
AVPe	+/–
Pe	+/–
MnPO	+
SChVL	+/–
SChDM	+/–

Area/nucleus	IL-18Rβ
VMPO	+/−
VLPO	+
VOLT	+/−
Anterior region	
LH	+(++)
AHA	+(++)
AHC	+(++)
AHP	+(++)
RCh	+/−
Circ	++
LA	+(++)
PaLM	++(+++)
PaDC	++(+++)
PaMP	+
PaMM	++
PaV	+(++)
PaPO	+
Tuberal region	
MCLH	+/−
DM	+(++)
DMD	+(++)
DMC	+(++)
DMV	+(++)
VMH	++
VMHDM	++(+++)
VMHC	++
VMHVL	++
TC	+
Arc	+(++)

Area/nucleus	IL-18Rβ
Mammillary region	
SMT	+(++)
SuMM	+
SuM	+/++
VTM	+
PH	+
DTM	+(++)
PMD	+
PMV	+
LM	++
ML	+
MM	+(++)
ME	+(++)
Mesenchephalon	
SuG	+
InG	+
DpG	+
PAG	+
IMLF	+(++)
APT	+/−
DpMe	+/−
RPC	++
RMC	++
DR	++
MnR	++
RLi	+/−
SNR	+
SNC	+
SNL	+

Area/nucleus	IL-18Rβ
VTA	+(++)
EW	+(++)
RMg	++
Rhomboencephalon	
Medulla oblungata	
SuVe	+
MVe	++
VCP	+(++)
DC	+(++)
Sp5ODM	++
Sp5OVL	++
Facial Nu 7	++
Gi	++
Cerebellum	
Deep cerebellar nuclei	
Lat; Med; Aint	+(++)
Cerebellar cortex	
Molecular layer	+/−
Purkinje cell layer	+++
Granular cell layer	+/−

Labelling intensity scale: −, not detected; +/− very low signal; +, weak signal; +(++) a weak to moderate signal; ++, moderate signal; ++(+++) a moderate to strong signal; +++, strong signal for IL-18Rβ mRNAs